Reports

Cretaceous Cold-Seep Communities and Methane-Derived Carbonates in the Canadian Arctic

Benoit Beauchamp, H. Roy Krouse, J. Christopher Harrison, Walter W. Nassichuk, Leslie S. Eliuk

Lower Cretaceous cold-seep fossil assemblages have been found in the Canadian Arctic Archipelago. Serpulid worm tubes and bivalves are most abundant in these communities; in contrast, fossils are scarce in the surrounding strata. The fossils are contained in an isotopically light ($\delta^{13}C = -25$ to -50 per mil) carbonate rock groundmass that is interpreted to have formed from bacterial oxidation of methane. The rocks were deposited at intermediate depth ($\leq$400 meters) in a cold marine environment; nearby normal faults may have provided a conduit for seeping methane and hydrogen sulfide needed to fuel chemosynthetic bacteria, and in turn, the higher life forms.

In recent years, chemosynthetic benthic communities (life oases) resembling hydrothermal vent-taxa but associated with cold hydrocarbon and brine seeps have been discovered at great (500 to 3300 m) (*1–4*) and intermediate (75 to 400 m) (*5–6*) depths in several oceans. Biologically, cold and hot chemosynthetic ecosystems are similar, as both types are based at the lowest trophic level on the bacterial oxidation of chemical compounds such as methane and hydrogen sulfide. In contrast, the geological processes responsible for the occurrence of either type of ecosystem are very different, and these differences are reflected in the associated geological products. Massive sulfide deposits are generally associated with hydrothermal vent communities (*7*), whereas isotopically light methane-derived authigenic carbonate occurs in association with nearly all known cold-seep communities, deep or shallow (*2, 5, 8–11*).

Ancient occurrences of chemosynthetic communities have been discovered in rocks ranging from Early Carboniferous to Early Tertiary in age (*12*). These communities are associated with massive sulfide deposits and have thus been interpreted as hydrothermal in origin. In this report, we describe cold-seep communities and associated methane-derived carbonates from Lower Cretaceous rocks in the Canadian Arctic. In addition to indicating that hydrocarbon-rich fluids seeped to the surface at some times and that oil or gas may still be present in the subsurface, these ancient cold-seep communities place their modern counterparts in a much broader temporal perspective, and may provide some clues as to how these communities and this geological association evolved (*13*).

Two Cretaceous seep communities occur on Ellef Ringnes Island (ERI), and two on Prince Patrick Island (PPI) (Fig. 1) (*14*), as mound-like carbonate rock units in the Christopher Formation, an Aptian to Albian siltstone and shale of the Sverdrup Basin and peripheral areas (*15*). The mounds are roughly circular, with diameters of 1, 3, 15, and 60 m, and they rise from 1 to 8 m above the surrounding ground. The mounds formed during deposition of the Christopher Formation, as indicated by Albian ammonites recovered from the ERI mounds. The PPI communities yielded bivalves of Early Cretaceous age (*16*). The Christopher Formation records a global sea level rise and an equivalent marine transgression. On ERI and PPI, the Christopher Formation was deposited in relatively deep prodelta to shelf environments (*15*), the bathymetry of which, however, probably did not exceed 400 m, as suggested by the presence of tiny red algal borings (*17*) in the ERI mounds.

The PPI seep communities developed in an active half graben that was one of many grabens forming the regionally extensive Eglinton graben, which developed adjacent to the Sverdrup Basin during the late Mesozoic (Fig. 1) (*18*). The graben with the PPI seep communities was active from Late Jurassic to, at least, Early Cretaceous time. Both PPI seep communities are situated along the growth fault that forms the edge of the local graben.

The ERI mounds are adjacent to a pair of normal faults that are spatially related to Hoodoo dome, a salt-cored diapir of the Carboniferous Otto Fiord Formation (*19*). These two faults likely formed in response to the formation of the salt dome. Doming started in Middle Triassic time (*20*), and by the Early Cretaceous, diapir-related topographic domes and fault scarps were widely developed on the sea floor of the Sverdrup Basin (*21*).

Fossils in the seep communities include abundant bivalves and serpulid worm tubes, associated with accessory ammonites, trochoid gastropods, foraminifers, and fish teeth. Terebratulid brachiopods (*Taimyrothyris*) are locally abundant, in association with coiled gastropods (*Spirorbis*) (*16*). Bivalves belong to the genera *Grammatodon* and *Nucula* (*16*) and average 1 cm in length; some reach 4 cm. Some millimeter-sized wood debris were also observed in the mounds; wood debris is a common component of the Christopher Formation in the

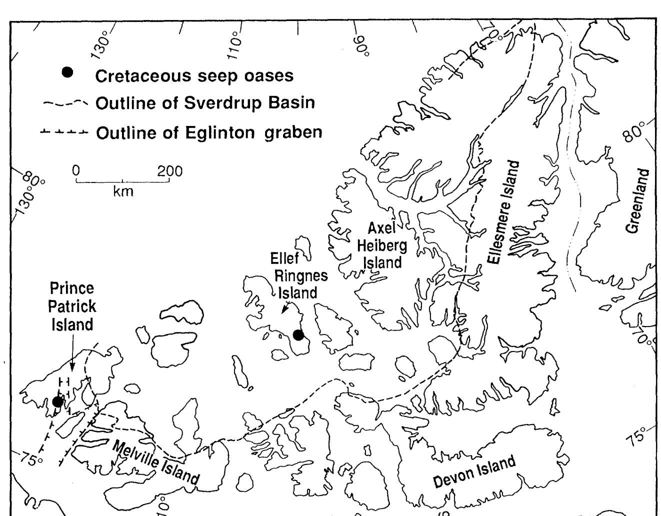

Fig. 1. Map of the northernmost islands of the Canadian Arctic Archipelago showing the outline of the Sverdrup Basin and Eglinton graben and the location of the Cretaceous cold-seep communities (oases) on Ellef Ringnes Island and Prince Patrick Island.

B. Beauchamp, J. C. Harrison, W. W. Nassichuk, Geological Survey of Canada, 3303 33rd Street Northwest, Calgary, Alberta, Canada T2L 2A7.
H. R. Krouse, Department of Physics, University of Calgary, Calgary, Alberta, Canada T2N 1N4.
L. S. Eliuk, Shell Canada Limited, Box 100, Station M, Calgary, Alberta, Canada T2P 2H5.

Sverdrup Basin (*15, 20*).

Two types of serpulids are present: the first type are relatively well-preserved tubes, 5 to 8 mm in diameter and up to 20 cm in length. These tubes have a dark brown, layered calcite wall, 100 to 200 μm in thickness. Many tubes are broken. The second type is represented by smaller tubes, 1 mm in diameter and up to 15 mm in length; the tube wall is at most 50 μm thick. The smaller tubes commonly occur in bundles of hundreds of tubes cemented to each other.

On both PPI and ERI, the carbonate rock that contains the seep communities comprises three early diagenetic authigenic carbonate phases: (i) a dark micrite, which is commonly brecciated and contains abundant organic matter, some pyrite framboids, and up to 10% by weight clay (*22*); ovoid fecal pellets, which range in length from 200 to 1000 μm, are also common in the micrite; (ii) a yellow calcite, which is associated with abundant pyrite, and invariably coats the serpulid tubes and various corrosion surfaces that developed early during diagenesis; and (iii) a pure, pyrite-free, botryoidal calcite, which fills most of the remaining porosity and alternates with layers of yellow calcite cement; relicts of thin calcite needles were observed in the botryoids. The relative proportions of the three carbonate phases vary greatly in the mounds, which are composed of various rock types, including lime mudstones, packstones, grainstones, and boundstones (*23*).

Fig. 2. Abundant serpulid worm tubes (arrows) cemented by botryoidal and yellow calcite from Ellef Ringnes Island. Micrite and fecal pellets can also be seen. Scale bar is 1.0 mm.

Most primary carbonate components from both the PPI and ERI mounds are characterized by low carbon isotope ratios [$\delta^{13}C$ (*24*)] from −25 to −50 per mil (Table 1). These values indicate that the carbonates are strongly depleted in ^{13}C relative to normal marine Albian fossils from Axel Heiberg Island (Table 1) and the Atlantic and Pacific oceans (*25*). The depletion of the PPI and ERI carbonate rocks is similar to that of methane-derived carbonate rocks from modern seep environments (Table 2) and other diagenetic settings (*26*).

Methane (CH_4) is the most ^{13}C-depleted carbon compound known: $\delta^{13}C$ for thermogenic CH_4 ranges from −35 to −50 per mil, $\delta^{13}C$ in biogenic CH_4 is less than −60 per mil (*27*). In contrast, $\delta^{13}C$ of dissolved inorganic carbon in marine waters ranges from −2 to 0 per mil (*28*). The oxidation of methane yields carbonate species (CO_2, HCO_3^-) that retain, to a large extent, the ^{13}C-depleted isotopic composition of methane. Extremely ^{13}C-depleted aragonite or calcite indicates that some of these methane-derived species were incorporated in the precipitating minerals, with or without the addition of carbon from other sources, such as dissolved inorganic carbon ($\delta^{13}C = -2$ to 0 per mil) or particulate organic carbon ($\delta^{13}C = -22$ to -30 per mil).

Table 1. Range and average (in brackets) of carbon and oxygen isotope ratios of carbonate components from Cretaceous seep communities on Prince Patrick Island (PPI) and Ellef Ringnes Island (ERI). Isotopes of Albian bivalve shells from Axel Heiberg Island (AHI) are also shown for comparison. Number of analyses is shown in brackets in the first column. Isotopic ratios are expressed relative to the PDB standard (*24*).

Component	$\delta^{13}C$ (per mil)	$\delta^{18}O$ (per mil)
	Prince Patrick and Ellef Ringnes seep communities	
Micrite		
PPI (2)	−47.6 to −40.0 (−43.8)	+0.5 to +0.7 (+0.6)
ERI (4)	−42.7 to −37.3 (−40.9)	−4.2 to −0.0 (−1.5)
Botryoidal calcite		
PPI (4)	−50.2 to −45.9 (−47.8)	−1.2 to +1.1 (−0.2)
ERI (17)	−44.7 to −36.0 (−40.1)	−3.2 to +1.0 (−0.4)
Yellow calcite		
PPI (1)	−42.3	+1.4
ERI (2)	−36.8 to −35.0 (−35.9)	−3.0 to −0.5 (−1.8)
Serpulid tube*		
PPI (2)	−44.0 to −43.0 (−43.5)	+0.8 to +1.2 (+1.0)
ERI (1)	−37.9	+0.1
Worm bundle†		
PPI (3)	−28.2 to −24.8 (−26.7)	+0.6 to +0.7 (+0.7)
Bivalve shell		
PPI (4)	−8.5 to −0.5 (−3.4)	−1.4 to +1.5 (−1.2)
	Normal marine Albian fossils	
Bivalve shell‡		
AHI (5)	+1.1 to +4.0 (+2.1)	−3.6 to −0.6 (−1.6)

*Material from several serpulid tubes is included in each analysis. †Only the cement crust (yellow and botryoidal calcite) cementing the tubes was analyzed; the tubes themselves are not preserved. ‡Shells come from the Christopher Formation at 79°03′N, 90°05′W.

Methane oxidation is a bacterially mediated process that can occur both in the aerobic and anaerobic diagenetic environments below the sediment-water interface. In anaerobic diagenetic environments, methane oxidation is coupled with sulfate reduction (*29*). In the North Sea, methane-derived, high-magnesium carbonate rocks that form in the sulfate-reduction zone and are associated with seeps are characteristically micritic, highly impure, and rich in pyrite and organic matter (*11*). These carbonate rocks are texturally and isotopically identical to the micritic limestone that occurs in association with the ERI and PPI seep communities.

Methane-derived aragonite botyroids also form in the surficial aerobic environment associated with the North Sea and Eastern Pacific seep communities (*2, 11*). Similar aragonite has also been reported from authigenic carbonate rocks of Pleistocene age offshore the northeastern United States (*26*). Aragonite rarely survives burial, and textural and indirect chemical evidence must be used to determine whether calcite cements in older rocks were originally aragonite (*30*). The ERI and PPI botryoids are thought to have recrystallized from aragonite because they are texturally and isotopically similar to the methane-derived aragonite botryoids associated with modern seep communities (*2, 11*).

All primary authigenic components from the ERI and PPP mounds have $\delta^{18}O$ values around 0 per mil (*24*) (Table 1). These components are slightly enriched relative to normal marine Albian bivalves from Axel Heiberg Island ($\delta^{18}O = -1.6$ per mil). In a similar fashion, modern authigenic carbonate from the Oregon subduction zone and the North Sea is enriched ($\delta^{18}O = +3$ to +8 per mil) (*2, 11*) relative to modern warm water carbonate (~0 per mil). Based on the temperature-dependent fractionation between carbonate and seawater (*31*), this enrichment suggests that the seep sites were cooler than the surrounding waters; it thus rules out a high temperature hydrothermal origin for the mounds.

The PPI and ERI seep communities and associated carbonates most likely formed through a sequence of events similar to those associated with pockmarks (*32*) in the

Table 2. Range and average (in parentheses) of carbon isotope ratios from authigenic carbonates associated with modern and Cretaceous seep communities. Number of analyses is indicated in parentheses in the location column. Isotopic ratios are expressed relative to the PDB standard. Entries without references are this report; MI = micrite; BC = botryoidal calcite; YC = yellow calcite.

Location	$\delta^{13}C$ (per mil)
Modern seep communities	
Oregon Subduction Zone* (20) (*2*)	−66.7 to −34.9 (−50.7)
North Sea pockmarks (14) (*11*)	−61.1 to −52.2 (−57.2)
Offshore Louisiana* (12) (*8*)	−47.5 to −14.5 (−30.6)
Florida Escarpment (?) (*9*)	>−48.5
Baffin Bay (?) (*5*)	−33.7 to −26.1
Cretaceous seep communities	
Prince Patrick Island	
MI, BC, YC (7)	−50.2 to −40.0 (−45.9)
BC, YC (3)†	−28.2 to −24.8 (−26.7)
Ellef Ringnes Island	
MI, BC, YC (23)	−44.7 to −35.0 (−39.8)

*$CaCO_3$ content > 25%. †From worm bundle capping southern mound.

North Sea (*6, 11*). We suggest that methane seeped to the surface along the faults and was then oxidized by bacteria in the sulfate-reduction zone, yielding ^{13}C-depleted CO_2. This CO_2 was incorporated in organic-rich, pyrite-containing, lime mud that formed in the surrounding clastic sediments. Excessive gas pressure beneath the newly formed carbonate crust led to its sudden brecciation and excavation, creating a pockmark-like depression on the sea floor. This carbonate crust provided a hardground that became populated by bivalves. Enhanced productivity at the seep site, undoubtedly catalyzed by the bacterial oxidation of methane, attracted a variety of higher organisms including gastropods and fish.

The occurrence of authigenic pyrite suggests that hydrogen sulfide (H_2S) also seeped from time to time. Seeping of H_2S would have led to acidic conditions on the sea floor, and the formation of the corrosion surfaces. At a high H_2S flux, local reducing conditions would develop and pyrite would precipitate on top of the corrosion surfaces and around the serpulid tubes. This interpretation is supported by recent observations of H_2S seeping near the Florida escarpment where bundles of living serpulids occur (*13*). At that site, H_2S seeping leads to considerable corrosion and dissolution of the surrounding carbonates and to extensive syndeposition of pyrite on the sea floor (*33*).

With a later decrease in the H_2S flux and the slow return to more alkaline, but still reducing conditions, pyrite- and organic-rich calcite crust (yellow high-Mg? calcite) could form on top of the corrosion surfaces and around the serpulid tubes. Aragonite precipitation would resume with the return to an H_2S-free aerobic environment.

The $\delta^{13}C$ of carbonate components indicates that methane-oxidizing bacteria were present below the sediment-water interface, and likely in the surrounding waters as well. By analogy with modern seep environments, a variety of grazing and filtering organisms must have fed directly on these bacteria. It may be significant that the $\delta^{13}C$ values of the PPI bivalve shells fall in the same range as symbiont-containing bivalves from modern cold-seep environments (*34*). The association of serpulid tubes and pyrite also suggests that the serpulids fed on sulfur-oxidizing bacteria. This suggestion is supported by the observation of serpulids at the H_2S seep site on the Florida escarpment, and near the H_2S hydrothermal vents of the Galapagos Rift and East Pacific Rise at 21° and 13°N (*35*). At that last locality, filamentous prokaryotic cells were observed connected to the wall of the midgut of some living serpulids (*35*).

The source of methane and H_2S that fed the PPI and ERI seep communities and led to precipitation of authigenic carbonate and pyrite is uncertain; in both areas, they could have been derived either from a deep thermogenic source or a shallow biogenic source (*36*). The carbon isotopes of carbonates are inconclusive because they can reflect more than one carbon source. In both areas, the fracture system associated with the nearby structures must have provided conduits for the CH_4 and H_2S. Diapir-associated fractures have been shown to provide the main conduits for seeping hydrocarbon in the Gulf of Mexico (*37*) and the North Sea (*6, 11*), two areas where chemosynthetic communities occur in association with methane-derived carbonates.

REFERENCES AND NOTES

1. M. C. Kennicutt II *et al.*, *Nature* **317**, 351 (1985); C. K. Paull *et al.*, *Science* **226**, 965 (1984).
2. L. D. Kulm *et al.*, *Science* **231**, 561 (1986).
3. L. A. Mayer, A. N. Shor, J. H. Clarke, D. J. W. Piper, *Deep Sea Res.* **35**, 1235 (1988).
4. A. Taira, K. Fujioka, K. Nakamura, *Eos* **67**, 1204 (1986).
5. A. C. Grant, E. M. Levy, K. Lee, J. D. Moffat, *Geol. Surv. Can. Pap.* **86-1A**, 65 (1986); R. Matsumoto, paper presented at the Annual Meeting of the Geological Association of Canada Mineralogical Association of Canada–Canadian Society of Petroleum Geologists, St. John's Newfoundland, 1988.
6. M. Hovland, A. Judd, G. Maisey, *New Sci.* **107**, 26 (1985).
7. J. C. Alt, P. Lonsdale, R. Haymon, K. Muehlenbachs, *Geol. Soc. Am. Bull.* **98**, 157 (1987).
8. J. M. Brooks *et al.*, *Org. Geochem.* **10**, 221 (1985).
9. A. C. Neumann, C. K. Paull, R. Commeau, J. Commeau, *Am. Assoc. Petrol. Geol. Bull.* **72**, 228 (1988).
10. S. Ritger, B. Carson, E. Suess, *Geol. Soc. Am. Bull.* **98**, 147 (1987); N. A. M. Schroeder, *Oreg. Geol.* **49**, 91 (1987).
11. M. Hovland, M. R. Talbot, H. Qvale, S. Olaussen, L. Aasberg, *J. Sediment. Petrol.* **57**, 881 (1987).
12. D. A. Banks, *Nature* **313**, 128 (1985); R. M. Haymon, R. A. Koski, C. Sinclair, *Science* **223**, 1407 (1984); C. Gaillard *et al.*, *Bull. Soc. Géol. France* **8**, 69 (1985); E. Oudin, J. Bouladon, J.-P. Paris, *C. R. Acad. Sci. Ser. B* **301**, 157 (1985); E. Oudin and G. Constantinou, *Nature* **308**, 349 (1984); P. H. von Bitter, S. D. Scott, P. E. Schenk, *Geol. Assoc. Can. Mineral. Assoc. Can. Can. Soc. Petrol. Geol. Progr. Abstr.* **13**, A130 (1988).
13. B. Hecker, *Bull. Biol. Soc. Wash.* **6**, 465 (1985).
14. Coordinates of the seep communities are: 75°08'00"N, 120°03'10"W (PPI); 76°12'22"N, 120°07'30"W (PPI); 78°10'N, 100°13'W (ERI).
15. A. F. Embry, *Geol. Surv. Can. Pap.* **85-1B**, 239 (1985).
16. Age and fossil determinations were performed by the late J. A. Jeletzky: *Geol. Surv. Can. Intern. Rep. Km-8-1974-JAJ; ibid. Km-5-1988-JAJ.*
17. C. M. Henderson, C. M. Styan, W. B. Styan, *Can. J. Earth Sci.* **19**, 1382 (1982).
18. J. C. Harrison, A. F. Embry, T. P. Poulton, *Geol. Surv. Can. Pap.* **88-1D**, 41 (1988).
19. W. W. Nassichuk and K. J. Roy, *ibid.* **75-1A**, 565 (1975).
20. H. R. Balkwill, *Geol. Surv. Can. Mem.* **390** (1983).
21. A. F. Embry, *Can. Soc. Petrol. Geol. Mem.* **8**, 189 (1982).
22. As determined by insoluble residues.
23. R. J. Dunham, *Am. Assoc. Petrol. Geol. Mem.* **1**, 108 (1962).
24. Carbon and oxygen isotopes were performed at the Laboratory of Stable Isotopes of the University of Calgary. Calcite components were dissolved in phosphoric acid at 25°C and then analyzed by mass spectrometry. Carbon and oxygen isotopes are expressed as δ values relative to the PDB standard:

$$\delta^{13}C = \left[\frac{(^{13}C/^{12}C)_{sample} - (^{13}C/^{12}C)_{standard}}{(^{13}C/^{12}C)_{standard}}\right] \times 1000$$

$$\delta^{18}O = \left[\frac{(^{18}O/^{16}O)_{sample} - (^{18}O/^{16}O)_{standard}}{(^{18}O/^{16}O)_{standard}}\right] \times 1000$$

25. A. G. Fischer and M. A. Arthur, *Soc. Econom. Paleontol. Mineral. Spec. Publ.* **25**, 19 (1977).
26. J. C. Hathaway and E. T. Degens, *Science* **165**, 690 (1969); H. H. Roberts and T. Whelan III, *Geochim. Cosmochim. Acta* **39**, 1085 (1975); C. S. Nelson and M. F. Lawrence, *Sedimentology* **31**, 645 (1984).
27. G. E. Claypool and I. R. Kaplan, in *Natural Gases in Marine Sediments*, I. R. Kaplan, Ed. (Plenum, New York, 1974), pp. 99–139; D. J. Frank, J. R. Gormly, W. M. Sackett. *Am. Assoc. Petrol. Geol. Bull.* **58**, 2319 (1974).
28. P. M. Kroopnick, *Deep Sea Res.* **32**, 57 (1985).
29. A. H. Devol and S. I. Ahmed, *Nature* **291**, 407 (1981); A. H. Devol, J. J. Anderson, K. Kuivila, J. W. Murray, *Geochim. Cosmochim. Acta* **48**, 993 (1984).
30. G. R. Davies, *Geology* **5**, 11 (1977).
31. S. Epstein, R. Buchsbaum, H. A. Lowenstam, H. C. Urey, *Geol. Soc. Am. Bull.* **62**, 417 (1951).
32. "Pockmarks" are local crater-like depressions that form in soft, fine-grained sea floor sediments, gener-

ally believed to result from gas and liquid expulsion (*11*).
33. C. K. Paull, *Geology* **15**, 545 (1987); R. F. Commeau *et al.*, *Earth Planet. Sci. Lett.* **82**, 62 (1985).
34. M. Rio *et al.*, *Bull. Soc. Géol. France* **8**, 151 (1985).
35. D. Desbruyères *et al.*, *Bull. Biol. Soc. Washington* **6**, 103 (1985).
36. Five pyrite samples from the ERI and PPI mounds yielded $\delta^{34}S$ values ranging from −8.1 to −20.7 per mil CDT (mean = −17.9 per mil), which is in the isotopic range of pyrite derived from bacterial sulphate reduction [H. R. Krouse, *Handbook of Environmental Isotope Geochemistry*, P. Fritz and J. C. Fontes, Eds. (Elsevier, Amsterdam, 1980), pp. 436–471].
37. E. W. Behrens, *Am. Assoc. Petrol. Geol. Bull.* **72**, 105 (1988); M. Hovland and J. H. Sommerville, *Mar. Petrol. Geol.* **2**, 319 (1985).
38. We thank the late J. A. Jeletzky for providing fossil determinations and A. F. Embry, D. Morrow, and two anonymous scientists for critically reviewing the manuscript. This research was supported by Energy, Mines, and Resources, Canada, The Polar Continental Shelf Project, and the Natural Science and Engineering Research Council of Canada.

13 October 1988; accepted 3 February 1989

Dynamics of Liquefaction During the 1987 Superstition Hills, California, Earthquake

T. L. Holzer, T. L. Youd, T. C. Hanks

Simultaneous measurements of seismically induced pore-water pressure changes and surface and subsurface accelerations at a site undergoing liquefaction caused by the Superstition Hills, California, earthquake (24 November 1987; M = 6.6) reveal that total pore pressures approached lithostatic conditions, but, unexpectedly, after most of the strong motion ceased. Excess pore pressures were generated once horizontal acceleration exceeded a threshold value.

Seismically induced liquefaction involves the loss of static shearing resistance of saturated, relatively loose, sandy deposits due to a tendency to closer packing of the constituent grains dynamically driven by seismic shear waves. If pore fluid in the liquefying layer cannot escape, this reduction in pore volume causes pore-water pressure to increase. Liquefaction is generally thought to occur when pore pressures approach lithostatic. Common surface manifestations of liquefaction include fountains of water laden with sediment and ground failure.

In this paper, we report simultaneous measurements of pore-water pressure change in a natural sand layer and earthquake shaking above and below the layer while it underwent liquefaction during the moment magnitude M = 6.6 (*1*) Superstition Hills earthquake (0515 PST, 24 November 1987). We also have such records for the preceding Elmore Ranch earthquake (1754 PST, 23 November 1987; M = 6.2) and aftershocks to each of these events (Table 1), none of which generated excess pore pressure. Understanding of liquefaction has been based primarily on laboratory investigations and post-earthquake field investigations (*2*). A few earlier measurements of pore pressure in loose sands during earthquakes have been made but not of the buildup of pore pressure to a lithostatic condition (*3*).

T. L. Holzer and T. C. Hanks, U.S. Geological Survey, 345 Middlefield Road, Menlo Park, CA 94025.
T. L. Youd, Department of Civil Engineering, Brigham Young University, Provo, UT 84602.

The engineering significance of liquefaction potential is enormous because many of the world's major cities are partly built upon young, saturated sediments. Understanding the mechanisms of liquefaction is also important in paleoseismology, because sand boils preserved in the geologic record have been used to date and to estimate magnitudes of prehistoric earthquakes (*4*). In the eastern United States, for example, ancient sand boils are the only reliable indicator of prehistoric earthquakes, in that surface fault scarps are absent—or, perhaps, have not yet been found—in this large region (*5*).

Our data come from an array of instruments deployed on and beneath the floodplain of the Alamo River in the Imperial Valley, California, a desert area that is heavily irrigated for crop cultivation (Fig. 1A). This site is 23 km east of the epicenter of the Elmore Ranch earthquake and 31 km east-northeast of the epicenter of the Superstition Hills earthquake. Our attention was drawn to the site when it experienced liquefaction during the Westmorland earthquake (26 April 1981; M = 5.9) (Fig. 1A). Instrumentation was installed in 1982 (*6*).

Shallow deposits at the array consist of saturated, floodplain sediments that fill an old incised channel of the Alamo River (*7*). The deposits probably date from catastrophic flooding of the river between 1905 and 1907 (*8*). The uppermost unit at the array is a 2.5-m-thick flat-lying silt bed that overlies the unit that liquefied, a 4.5-m-thick silty sand (Fig. 1B). The fines content (<75 μm) of the silty sand averages 33% and ranges from 16 to 60%; porosity is about 41%. Beneath these floodplain deposits is a 5-m-thick silty clay unit, the uppermost unit of a dense and regionally extensive sedimentary deposit. The Alamo River, a perennial stream because of drainage from irrigation, currently occupies a 3.7-m-deep channel 23 m east of the center of the array and controls the water table depth at about 1.2 m. Despite the shallow water table, the land surface usually is arid because of the desert conditions.

Six pore-water pressure transducers and two three-component force-balance acceler-

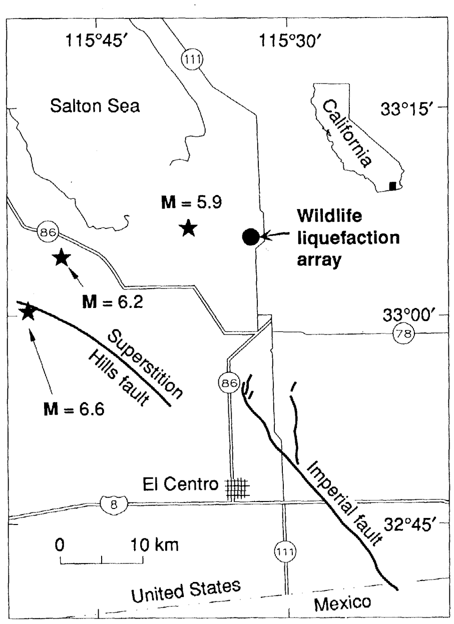

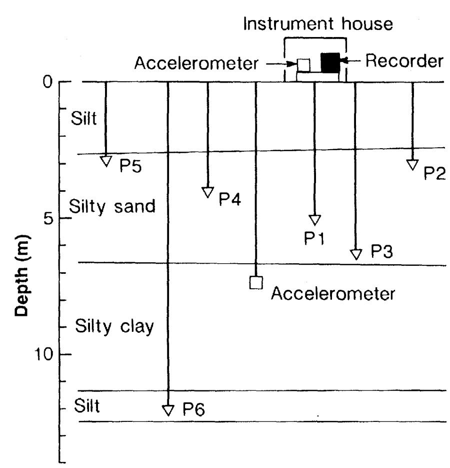

Fig. 1. (**Left**) Location map of liquefaction array and earthquake epicenters. M = 6.6 is the Superstition Hills earthquake, M = 6.2 is the Elmore Ranch earthquake, and M = 5.9 is the Westmorland earthquake. (**Right**) Stratigraphic cross section of array and schematic of instrument deployment. In plan view, pore-pressure transducers (denoted by P) are equally spaced on the perimeter of a circle with a diameter of 9.1 m. Accelerometers are near center of circle (*7*).